

# Differentiation of hemangioblastomas from pilocytic astrocytomas using 3-T magnetic resonance perfusion-weighted imaging and MR spectroscopy

D. J. She · Z. Xing · Z. Zeng · X. Y. Shang · D. R. Cao

Received: 17 October 2014 / Accepted: 27 November 2014 / Published online: 7 December 2014  
© Springer-Verlag Berlin Heidelberg 2014

## Abstract

**Introduction** Hemangioblastomas and pilocytic astrocytomas (PAs) present similar imaging features on conventional MR imaging, making differential diagnosis a challenge. The purpose of this study was to evaluate the usefulness of dynamic susceptibility-weighted contrast-enhanced perfusion-weighted imaging (DSC-PWI) and proton MR spectroscopic imaging in the differentiation of hemangioblastomas and PAs. **Methods** A 3.0-T MR imaging unit was used to perform DSC-PWI and conventional MR imaging on 14 patients with hemangioblastomas and 22 patients with PAs. Four patients with hemangioblastomas and 10 PA patients also underwent proton MR spectroscopy. Parameters of relative peak height (rPH) and relative percentage of signal intensity recovery (rPSR) were acquired by DSC-PWI and variables of N-acetylaspartate (NAA)/creatine (Cr), choline (Cho)/Cr, and lactate-lipid (Lac-Lip)/Cr by MR spectroscopy. The sensitivity, specificity, and the area under the receiver operating characteristic curve of all analyzed parameters at respective cutoff values were determined.

**Results** Higher rPH but lower rPSR values were detected in hemangioblastomas compared to PAs. The NAA/Cr ratio was significantly lower in hemangioblastomas compared with PAs. The threshold values  $\geq 3.2$  for rPH provide sensitivity, specificity, positive predictive values, and negative predictive values of 85.7, 95.5, 92.3, and 91.3 %, respectively, for differentiating hemangioblastomas from PAs. The optimal

threshold values were  $\leq 0.9$  for rPSR and  $\leq 1.5$  for NAA/Cr ratios in tumor.

**Conclusion** Significantly higher rPH and lower NAA/Cr were seen in patients with hemangioblastomas when compared with PA patients, suggesting that DSC-PWI and proton MR spectroscopy are helpful in the characterization and differentiation of these two types of tumors.

**Keywords** Dynamic susceptibility-weighted contrast-enhanced perfusion-weighted imaging · Proton MR spectroscopic imaging · Hemangioblastoma · Pilocytic astrocytoma

## Introduction

Hemangioblastomas and pilocytic astrocytomas (PAs) are two types of brain tumors most commonly occur in the cerebellum. Hemangioblastomas and PAs are both benign in nature and are classified as grade I according to the World Health Organization [1]. They are potentially curable by surgical resection and are associated with a longer survival [2, 3]. However, hemangioblastomas are more vascular than PAs, which has important surgical and clinical implication. The surgical resection of hemangioblastomas could lead to high mortality and morbidity rates, which is often related to the complication of excessive bleeding [4, 5]. Thus, a reliable preoperative differentiation between them is important. Unfortunately, the two entities cannot be reliably distinguished on conventional magnetic resonance imaging (MRI) because of their similar imaging findings and locations, typically appearing as a cystic mass with an enhancing mural nodule in the cerebellum [3, 6].

Given that differentiation of hemangioblastomas and PAs is challenging to radiologists, advanced MR imaging techniques including dynamic susceptibility-weighted contrast-

D. J. She · Z. Xing · Z. Zeng · D. R. Cao (✉)  
Department of Radiology, First Affiliated Hospital of Fujian Medical University, 20 Cha-Zhong Road, Fuzhou, Fujian 350005, People's Republic of China  
e-mail: dairongcao@163.com

X. Y. Shang  
Department of Medicine and the Moores UCSD Cancer Center,  
University of California, San Diego, La Jolla, CA, USA

enhanced perfusion-weighted imaging (DSC-PWI) and proton MR spectroscopy (MRS) can supplement physiological and metabolic information to the anatomical MR imaging. The perfusion-weighted imaging that provides the noninvasive morphologic and functional status of the tumor microvasculature can be helpful in the preoperative evaluation and grading of brain tumors [7–9]. MR measurement of relative cerebral blood volume (rCBV) has become one of the most robust and standard hemodynamic variable used in the characterization of the brain tumors. However, the rCBV measurements are often complicated by disruption or lack of a blood-brain barrier within the tumor vessels, which requires a correction for the overestimation or underestimation of rCBV consequent to contrast material leakage during the first pass [10]. Moreover, rCBV measurements do not provide any information on capillary permeability. Two new hemodynamic variables derived from DSC-PWI, the peak height (PH) and the percentage of signal intensity recovery (PSR) have been shown to provide additional information on tumor capillary volume and capillary permeability [11, 12], respectively. MR spectroscopy provides complementary metabolic and histologic marker information about brain tumors, which may distinguish brain tumors and assist in tumor grading [13, 9, 14]. Although hemangioblastomas mimic PAs in their imaging appearance on conventional MRI, a large body of evidence has demonstrated that hemangioblastomas present histologic aspects and tumor origin very distinct from those found in pilocytic astrocytomas. Thus, application of advanced MR imaging techniques may have a better chance to assess and distinguish the functional and metabolic differences occurring between hemangioblastomas and pilocytic astrocytomas.

There are a few reports that evaluated the advanced MR imaging features of hemangioblastomas with respects to capillary volume and permeability on DSC-PWI [15, 16] and metabolism on MRS [17]. The purpose of this study was to determine whether 3-T MR spectroscopy and DSC-PWI can be used to differentiate between hemangioblastomas and PAs on the basis of differences in metabolite levels and microvasculature in the tumor.

## Materials and methods

### Patients

The Institutional Review Board of our hospital approved this retrospective study and patient informed consent was waived. MR imaging examinations (conventional, DSC-PWI, and MR spectroscopy) were performed from July 2010 to July 2014. The presence of the hemangioblastomas or PAs was histologically confirmed after surgical resection. Patients with previously treated,

multiple brain lesions, or nonenhancing tumor were excluded. MR imaging studies of 36 patients were reviewed. Fourteen patients had hemangioblastomas (7 men, 7 women, aged 21–64 years with a mean age,  $39.1 \pm 14.8$  years), and 22 had PAs (13 men, 9 women, aged 3–49 years with a mean of  $17.8 \pm 11.0$  years). MR spectroscopy was performed on 4 patients with hemangioblastomas and 10 patients with PAs.

### MR techniques

The examinations were performed in the routine clinical workup by using a 3-T MR scanner (Magnetom Verio TIM; Siemens Healthcare, Germany) with an 8-channel head matrix coil. The conventional MR imaging protocol consisted of the following sequences: transverse T1-weighted spin-echo imaging (TR/TE 250 ms/2.48 ms), transverse T2-weighted turbo spin-echo imaging (TR/TE 4000 ms/96 ms), transverse fluid-attenuated inversion recovery (FLAIR; TR 9000, TE 94, TI 2500 ms) and three-planes contrast-enhanced gradient-echo T1-weighted imaging (TR/TE 250 ms/2.48 ms) which was acquired following the acquisition of DSC-PWI sequences. It was uniform in all sequences about the field of view (FOV) at  $220 \times 220$  mm, slice thickness of 5 mm, and intersection gap of 1.0 mm.

The DSC-PWI was performed with a gradient-recalled T2\*-weighted echo-planar imaging sequence. The imaging parameters used were as follows: TR/TE = 1000–1250/54 ms, flip angle =  $35^\circ$ , NEX = 1.0, FOV =  $220 \times 220$ , slice thickness = 5 mm, and intersection gap = 1.0 mm. During the first three phases, images were scanned before injecting the contrast agent to establish a precontrast baseline. When the scan was to the fourth phase of DSC-PWI, 0.1 mmol/kg body weight of gadopentetate dimeglumine (GD-DTPA) was injected with an MR-compatible power injector at a rate of 5 ml/s through an intravenous catheter placed in the antecubital vein, followed immediately by a 20-ml continuous saline flush. The series of 20 sections, 60 phases, and 1200 images were acquired in 1 min and 36 s.

Single-voxel MR spectroscopy of the tumor was acquired after administration of GD-DTPA in 4 patients with hemangioblastomas and 10 patients with PAs. Using the contrast-enhanced T1 sequence as reference for voxel placement, single-voxel proton MR spectroscopy was performed with point-resolved spatially localized spectroscopy (PRESS) technique: TR 2000 ms, a short TE (30 ms), NEX 3, scan time 2 min and 33 s. A region of interest at 2 to  $8 \text{ cm}^3$ , depending on the size of the lesion, was placed on the enhancing parts of the tumors with the aim of minimizing any partial volume surrounding normal-appearing tissue.

## Data processing

Image postprocessing of perfusion data and perfusion measurements was performed on an off-line SIEMENS workstation with standard software. To obtain maximum peak height and maximum percentage of signal intensity recovery values, four small round regions of interest (ROI) (size 30–40 mm<sup>2</sup>) were used. Regions of interest were placed on the original gray-scale perfusion maps overlaid on enhancing tumor on contrast-enhanced T1- and susceptibility-weighted images. Contrast-enhanced T1- and susceptibility-weighted images were used to ensure that ROI did not include necrotic, cystic, hemorrhagic, or apparent blood vessel regions. This means for the measurements of maximal abnormality provide the highest interobserver and intraobserver reproducibility in rPH and rPSR measurements [18]. To acquire relative (normalized) values, all perfusion measurements from the tumors were divided by values from the unaffected white matter of the contralateral hemisphere. The T2\*-weighted signal intensity curves acquired for the regions of interest were analyzed. For the T2\*-weighted signal intensity curves, three major points were identified: SI<sub>post</sub>—the signal intensity at the end of the DSC-PWI process, SI<sub>min</sub>—the signal intensity at the minimum of the signal intensity-time curve after contrast arrival, and SI<sub>pre</sub>—the signal intensity at precontrast baseline. The PSR was calculated with the following equation by Cha et al. [9, 7]:  $PSR = (SI_{post} - SI_{min}) / (SI_{pre} - SI_{min}) \times 100\%$ , while the PH was calculated using the following equation:  $PH = SI_{min} - SI_{pre}$ .

The MR spectroscopy data processing was performed on an off-line workstation with standard software (SIEMENS). Postprocessing steps including frequency shift, base-line correction, phase correction, peak fitting, and peak analysis were performed automatically. The region between 0.2 and 4.0 ppm of the spectra was analyzed, and the following metabolite concentrations were evaluated: N-acetylaspartate (NAA) at 2.02 ppm; creatine (Cr) at 3.02 ppm; choline (Cho) at 3.22 ppm; lactate-lipid (Lac-Lip) at 0.5–1.5 ppm. The peak area measurements were used to calculate NAA/Cr, Cho/Cr, and Lac-Lip/Cr ratios.

## Data analysis

All pilocytic astrocytomas and hemangioblastomas parameters are presented as means±standard deviation (SD). A non-parametric Mann-Whitney statistical test was applied to test the differences in terms of quantitative variances between the hemangioblastoma and PA groups. The receiver operating characteristic analysis curve (ROC) was performed to decide optimum thresholds and diagnostic accuracy of MRS, rPH, and rPSR for differentiating hemangioblastomas from PAs. The sensitivity, specificity, positive predictive value (PPV), negative predictive value (NPV), and cutoff value associated

with each parameter of DSC-PWI and MRS as a function of the threshold value were calculated to differentiate hemangioblastomas from PAs. The cutoff values chosen were those that provided highest sensitivity and specificity jointly.

Statistical analysis was performed in the Statistical Package for the Social Sciences, Version 17.0 (Chicago, IL, USA). A *P* value less than 0.05 was statistically significant.

## Results

The main clinical and radiographic features of hemangioblastomas and PAs in this study are summarized in Table 1.

The maximum value of rPH and rPSR, calculated for hemangioblastomas and PAs are shown in Table 2 and Fig. 1. The rPH<sub>max</sub> in patients with hemangioblastomas was significantly higher than in those with PAs (5.0±2.7 versus 2.0±0.9, *P*<0.001). All lesions in the hemangioblastomas group (100 %) displayed markedly elevated perfusion, while only 9/22 (41 %) PAs showed mildly increased perfusion (rPH>2.0). From the ROC analysis, with a threshold value of ≥3.2 for rPH, the sensitivity, specificity, and accuracy in the diagnosis of hemangioblastomas were 85.7, 95.5, and 91.7 %, respectively.

In analyzing the percentage of signal intensity recovery, there was a statistically significant difference between the hemangioblastoma group and the PA group as noted in Table 2 and Fig. 1. The signal intensity in 14 PAs cases (14/22, 64 %) exceeded that of the baseline after the first pass, whereas none of hemangioblastoma group exceeded the baseline even at the

**Table 1** The main clinical and radiographic features of hemangioblastomas and pilocytic astrocytomas

	Hemangioblastomas	Pilocytic astrocytomas
Number of patients(male/female)	14(7/7)	22(13/7)
Age	39.1±14.8	17.8±11.0
Localization		
Cerebellum	11	8
Cerebrum	2	3
Optic chiasm		1
Pons		6
Basal ganglia		1
Thalamus		2
Medulla	1	
Lateral ventricular		1
MR appearance		
Cyst and nodule	9	15
Solid with central cyst	5	7

**Table 2** Comparison of the PA and HGA groups with regard to the variables of interest (mean±SD)

	Hemangioblastomas	Pilocytic astrocytomas	P value
rPH	5.0±2.7	2.0±0.9	<0.001
rPSR	0.5±0.3	1.0±0.3	<0.001
NAA/Cr	0.9±0.6	2.1±1.1	0.036
Cho/Cr	2.2±2.8	2.4±2.1	0.304
Lac-Lip/Cr	5.6±4.5	4.5±5.9	0.635

end of the DSC imaging process. The relative percentage of signal intensity recovery in hemangioblastomas was significantly lower than that in PAs ( $0.5\pm 0.3$  versus  $1.0\pm 0.3$ ;  $P<0.001$ ). A threshold value of  $\leq 0.9$  for rPSR optimized differentiation of hemangioblastomas and PAs with the sensitivity, specificity and accuracy of 85.7 %, 81.8 % and 83.3 %, respectively.

The NAA/Cr values in the PA group were significantly higher than those in the hemangioblastoma group (Table 2 and

Fig. 2). There were no statistically significant differences between the hemangioblastoma and PA groups in the remaining metabolite ratios.

The sensitivity, specificity, PPV, NPV, and accuracy of each MR imaging parameters for differentiation between respective threshold values are shown in Table 3.

## Discussion

In this study, we used multiple diagnostic parameters obtained with DSC-PWI and MRS for possible preoperative differentiation of hemangioblastomas and PAs, both of which can have similar appearance on conventional MR imaging. Our data showed that patients with hemangioblastomas demonstrated significantly higher rPH, lower rPSR values, and lower NAA/Cr ratios as compared with PAs.

The peak height, as its name applies, is defined as the maximal signal intensity drop from the precontrast baseline

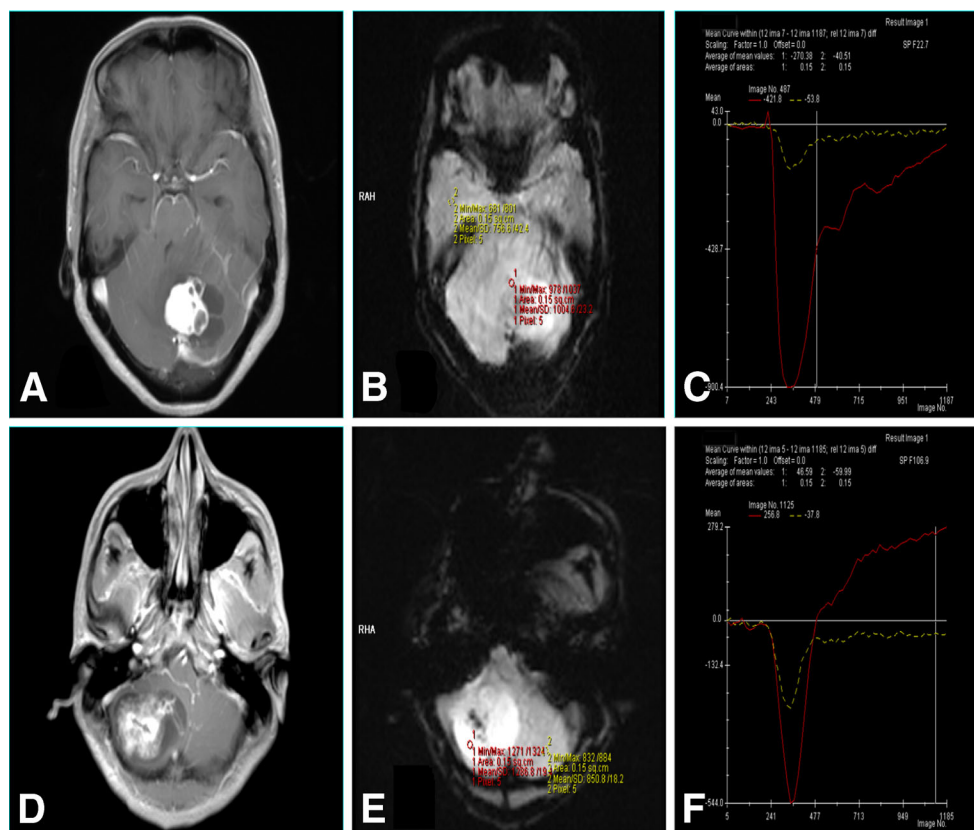
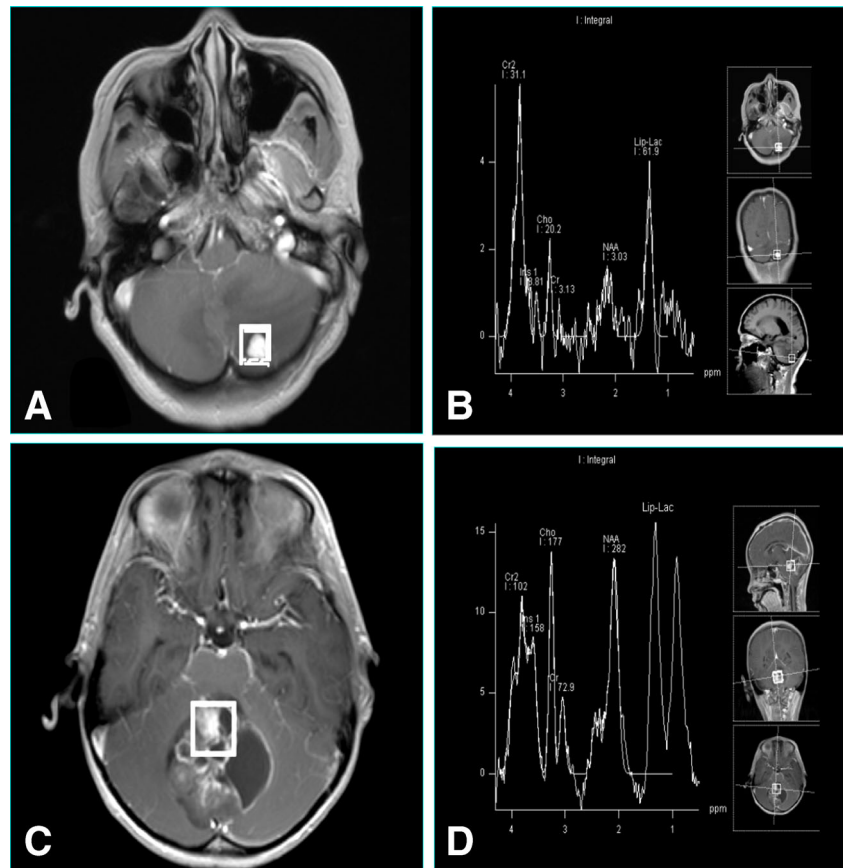


**Fig. 1** Comparison of rPH and rPSR between hemangioblastoma and pilocytic astrocytoma on PWI. **b, e** Original gray-scale perfusion maps used for positioning of the regions of interest in the tumor. **a–c** A 44-year-old woman with a solid-cystic hemangioblastomas in the left cerebellar hemisphere. **a** Axial contrast-enhanced T1-weighted imaging showed intense homogeneous enhancement in the solid portion of the tumor and lack of enhancement of the cystic portion. **b, c** The red region of interest placed on the enhancing lesion to measure the maximum signal-

intensity recovery showed a rapid steep signal drop with a tendency returning to baseline, followed by a second, smaller dip. **d–f** A 23-year-old man with a solid-cystic pilocytic astrocytomas in the right cerebellar hemisphere. **d** Axial contrast-enhanced T1-weighted imaging showed intense inhomogeneous enhancement in the solid portion of the tumor. **e, f** The red region of interest placed on the enhancing tumor to measure the maximum signal-intensity recovery demonstrated the overshooting of the baseline on the recovery maps

**Fig. 2** Comparison of NAA/Cr, Cho/Cr, and Lac-Lip/Cr ratios on short-TE single-voxel MR spectroscopy in hemangioblastomas and pilocytic astrocytomas. **a, c** Axial contrast-enhanced T1-weighted imaging was used for positioning of the regions of interest in the tumor.

**a, b** The solid homogenous enhancing hemangioblastoma in the left cerebellar hemisphere had a NAA peak. **c, d** Cystic solid pilocytic astrocytomas located in the cerebellar vermis also had an NAA peak (**d**), but the NAA/Cr ratio in this tumor was higher than that found in the hemangioblastomas (**b**)



during the bolus phase of the first pass of contrast agent. rPH has been shown to correlate with rCBV [8] and thus reflect total tumor capillary volume. Our finding that rPH was significantly increased in hemangioblastomas is in a good agreement with a previous observation showing the marked elevation of rCBV in hemangioblastomas [15, 19]. The differences in either rCBVs or rPH between hemangioblastomas and PAs may be explained by distinct histological features of the two tumor types. Hemangioblastomas have abundant tumor vessels within lesions owing to strong expression of vascular endothelial growth factors [20, 21], whereas PAs are sparsely vasculatured in a wide interstitial space [22]. Furthermore, the

results of this study also demonstrated that rPH is a robust parameter with high sensitivity (85.7 %) and specificity (95.5 %) which would aid in differentiating hemangioblastomas from PAs.

PSR is influenced by many factors including the permeability of capillaries, the amount of contrast agent leakage, the rate of blood flow, as well as the size of extravascular space [8, 9]. In our study, 64 % PA (14/22) showed that the signal time-intensity curves crossed the baseline after the first pass, which is consistent with those reported by Grand et al. [16]. In contrast, all hemangioblastomas except one case exhibited a distinct pattern of signal time-intensity curves characterized by a rapid steep signal drop with a tendency returning to baseline followed by a second but smaller dip. We found the relative PSR at contrast-enhancing areas of hemangioblastomas markedly lower than those in PAs. The signal intensity for DSC-PWI is well known to be the combined result of complex T1- and T2\*-shortening effect from the accumulation of contrast agent in the interstitial space of lesion. The T1 effects caused higher signal-intensity recovery, whereas the T2\* effects lead to the opposite. When the T1-shortening effects, due to accumulation of contrast agent in the interstitial space, overwhelm the T2\*-shortening effects, the signal intensity increases and even exceed the baseline level. In a study by Paulson et al. [23], the signal intensity overshoot

**Table 3** Cutoff values, sensitivity, specificity, positive predictive value, negative predictive value, and accuracy of the different MRI parameters to identify hemangioblastomas

	Threshold value <sup>a</sup>	Sensitivity (%)	Specificity (%)	PPV (%)	NPV (%)	Accuracy (%)
rPH	≥3.2	85.7	95.5	92.3	91.3	91.7
rPSR	≤0.9	85.7	81.8	75	90	83.3
NAA/Cr	≤1.5	100	70	57.1	100	78.6

PPV positive predictive value, NPV negative predictive value

<sup>a</sup> Hemangioblastoma group

from baseline was explained as T1 leakage effects resulting from the contrast agent extravasation. The significant difference in the rPSR between hemangioblastomas and PAs in this study may suggest that contrast agent leakage into the interstitial space in PAs is more pronounced than that in hemangioblastomas. In most PAs, domination of T1 effects may derive from the abundant leakage of contrast agent causing the signal increase above the baseline. However, T2\* leakage effects were more evident in hemangioblastomas with the signal not returning to the baseline. In addition, the tumor vessels in hemangioblastomas often show cavernous appearance [21] that may cause the reduction in blood flow rate, and possibly the tumor with low blood flow rate might have a lower recovery of the signal. However, T2\* and T1 effects of contrast agent in the extravascular space are complex and can be affected by many factors such as the permeability of capillaries, the amount of contrast agent leakage, the rate of blood flow, as well as the size of extravascular space, leading to different PSR [8, 9]. The high max rPSR (overshoot from baseline) appeared to be indicative of PAs, while a low max rPSR was very suggestive of hemangioblastomas. It may be worth noting that 14 cases of infratentorial PAs and 8 cases of supratentorial PAs recruited in the study presented similar imaging characteristics, and there was no significant difference in the parameters of rPH and rPSR between the PAs located in the posterior fossa and in the supratentorial region (data not shown).

Proton MR spectroscopy can be used to acquire information on the metabolism of brain tissue [17, 24]. NAA is generally thought to present in high concentrations in the normal neurons and axons, and its presence may be an indirect marker for tumor composition according to the density of residual neuronal cells within a tumor. Cho has been recognized as a main component of membranes and could reflect the rate of cellular membrane turnover and cellular density. Lactate is an end product of the anaerobic glycolytic cycle whose concentrations within a tumor may indicate the tumor necrosis [25, 17]. The presence of lipids has been recognized to originate from mobile lipid molecules as a result of tissue necrosis and degradation [26]. To our knowledge, there are no reports in the literature on the application of MRS to differentiate hemangioblastomas from pilocytic astrocytomas. In this study, we found that only NAA/Cr ratios in hemangioblastomas were significantly lower than those in PAs among all metabolite ratios analyzed. The NAA/Cr ratio was decreased in both tumor types but much lower in hemangioblastomas, which might be due to the different histogenesis and histological behavior between the two tumor types. PAs have been recognized to rise through the neural axis with infiltrative nature, whereas hemangioblastomas are mainly composed of stromal cells of incompletely differentiated, non-neuronal, and yet neuroectodermal nature [27]. Furthermore, hemangioblastomas are usually well circumscribed

and rarely infiltrate adjacent brain tissues [21]. Consistently, this study showed that hemangioblastomas have no neuronal cells or low attenuation of residual neuronal cells with the lesions compared with pilocytic astrocytomas. In particular, NAA was observed only in one case of hemangioblastomas in our study, a phenomenon consistent with an MRS study of a patient of hemangioblastomas reported by Isobe et al. [28]. Although necrosis is seldom found in PAs and hemangioblastomas [17], we found Lac-Lip/Cr ratios increased in both tumor types irrespective of no statistically significant difference between them. The presence of Lac-Lip in PAs without necrosis may be explained by mitochondrial dysfunction [17], while in hemangioblastomas, it may be attributed to lip droplets contained in stromal cells [21].

Our study has a few limitations. The most significant limitation of this study was its retrospective nature, which may have led to bias in patient selection and the small population of cases with MRS examination, especially for the hemangioblastoma groups with only four patients. Another limitation of this study was that we chose a short TE of 35 ms for MRS, which may have the possibility, if any, of being not able to separate the lactate peak from the lipid peak because both appear at 1.33 ppm above the baseline. Further prospective studies with a larger number of cases are warranted. Lastly, although single-voxel MRS employed in this study could give a better signal-to-noise ratio with a shorter acquisition time as compared with multivoxel MRS technique, it may overlap a solid component of brain tumors with a cystic one or normal brain tissue and precise positioning of a voxel after data acquisition is not allowed.

## Conclusions

To the best of our knowledge, this is the first demonstration to date that dynamic susceptibility perfusion-weighted and spectroscopic MR measurements in the enhancing tumoral region were able to differentiate hemangioblastomas from pilocytic astrocytomas. Higher rPH and lower rPSR values appear to favor a diagnosis of hemangioblastomas, while higher NAA/Cr ratios in tumor favor a diagnosis of pilocytic astrocytomas.

**Ethical standards and patient consent** We declare that all human studies have been approved by the Institutional Review Board of First Affiliated Hospital of Fujian Medical University and have therefore been performed in accordance with the ethical standards laid down in the 1964 Declaration of Helsinki and its later amendments. Due to the retrospective nature of this study, the Institutional Review Board waived patient consent.

**Conflict of interest** We declare that we have no conflict of interest.

## References

- Louis DN, Ohgaki H, Wiestler OD, Cavenee WK, Burger PC, Jouvet A, Scheithauer BW, Kleihues P (2007) The 2007 WHO classification of tumours of the central nervous system. *Acta Neuropathol* 114(2): 97–109. doi:10.1007/s00401-007-0243-4
- Catapano D, Muscarella LA, Guarnieri V, Zelante L, D'Angelo VA, D'Agruma L (2005) Hemangioblastomas of central nervous system: molecular genetic analysis and clinical management. *Neurosurgery* 56(6):1215–1221, discussion 1221
- Koeller KK, Rushing EJ (2004) From the archives of the AFIP: pilocytic astrocytoma: radiologic-pathologic correlation. *Radiographics : Rev Publ Radiol Soc N Am Inc* 24(6):1693–1708. doi:10.1148/rg.246045146
- Brundl E, Schodel P, Ullrich OW, Brawanski A, Schebesch KM (2014) Surgical resection of sporadic and hereditary hemangioblastoma: our 10-year experience and a literature review. *Surg Neurol Int* 5:138. doi:10.4103/2152-7806.141469
- Padhi S, Sarangi R, Challa S, Bussary P, Panigrahi MK, Purohit AK (2011) A 10-year retrospective study of hemangioblastomas of the central nervous system with reference to von Hippel-Lindau (VHL) disease. *J Clin Neurosci Off J Neurosurg Soc Australasia* 18(7):939–944. doi:10.1016/j.jocn.2010.12.050
- Erridge SC, Hart MG, Kerr GR, Smith C, McNamara S, Grant R, Gregor A, Whittle IR (2011) Trends in classification, referral and treatment and the effect on outcome of patients with glioma: a 20 year cohort. *J Neurooncol* 104(3):789–800. doi:10.1007/s11060-011-0546-0
- Bladowska J, Zimny A, Guzinski M, Halon A, Tabakow P, Czyz M, Czapiga B, Jarmundowicz W, Sasiadek MJ (2013) Usefulness of perfusion weighted magnetic resonance imaging with signal-intensity curves analysis in the differential diagnosis of sellar and parasellar tumors: preliminary report. *Eur J Radiol* 82(8):1292–1298. doi:10.1016/j.ejrad.2013.01.033
- Mangla R, Kolar B, Zhu T, Zhong J, Almast J, Ekholm S (2011) Percentage signal recovery derived from MR dynamic susceptibility contrast imaging is useful to differentiate common enhancing malignant lesions of the brain. *AJNR Am J Neuroradiol* 32(6):1004–1010. doi:10.3174/ajnr.A2441
- Cha S, Lupo JM, Chen MH, Lamborn KR, McDermott MW, Berger MS, Nelson SJ, Dillon WP (2007) Differentiation of glioblastoma multiforme and single brain metastasis by peak height and percentage of signal intensity recovery derived from dynamic susceptibility-weighted contrast-enhanced perfusion MR imaging. *AJNR Am J Neuroradiol* 28(6):1078–1084. doi:10.3174/ajnr.A0484
- Heiland S, Benner T, Debus J, Rempp K, Reith W, Sartor K (1999) Simultaneous assessment of cerebral hemodynamics and contrast agent uptake in lesions with disrupted blood-brain-barrier. *Magn Reson Imaging* 17(1):21–27
- Barajas RF Jr, Chang JS, Segal MR, Parsa AT, McDermott MW, Berger MS, Cha S (2009) Differentiation of recurrent glioblastoma multiforme from radiation necrosis after external beam radiation therapy with dynamic susceptibility-weighted contrast-enhanced perfusion MR imaging. *Radiology* 253(2):486–496. doi:10.1148/radiol.2532090007
- Lupo JM, Cha S, Chang SM, Nelson SJ (2005) Dynamic susceptibility-weighted perfusion imaging of high-grade gliomas: characterization of spatial heterogeneity. *AJNR Am J Neuroradiol* 26(6):1446–1454
- Yang D, Korogi Y, Sugahara T, Kitajima M, Shigematsu Y, Liang L, Ushio Y, Takahashi M (2002) Cerebral gliomas: prospective comparison of multivoxel 2D chemical-shift imaging proton MR spectroscopy, echoplanar perfusion and diffusion-weighted MRI. *Neuroradiology* 44(8):656–666. doi:10.1007/s00234-002-0816-9
- Orphanidou-Vlachou E, Auer D, Brundler MA, Davies NP, Jaspan T, MacPherson L, Natarajan K, Sun Y, Arvanitis TN, Grundy RG, Peet AC (2013) (1)H magnetic resonance spectroscopy in the diagnosis of paediatric low grade brain tumours. *Eur J Radiol* 82(6):e295–e301. doi:10.1016/j.ejrad.2013.01.030
- Bing F, Kremer S, Lamalle L, Chabardes S, Ashraf A, Pasquier B, Le Bas JF, Krainik A, Grand S (2009) Value of perfusion MRI in the study of pilocytic astrocytoma and hemangioblastoma: preliminary findings. *J Neuroradiol J Neuroradiol* 36(2):82–87. doi:10.1016/j.neurad.2008.09.002
- Grand SD, Kremer S, Tropres IM, Hoffmann DM, Chabardes SJ, Lefournier V, Berger FR, Pasteris C, Krainik A, Pasquier BM, Peoch M, Le Bas JF (2007) Perfusion-sensitive MRI of pilocytic astrocytomas: initial results. *Neuroradiology* 49(7):545–550. doi:10.1007/s00234-006-0204-y
- Hwang JH, Egnaczyk GF, Ballard E, Dunn RS, Holland SK, Ball WS Jr (1998) Proton MR spectroscopic characteristics of pediatric pilocytic astrocytomas. *AJNR Am J Neuroradiol* 19(3):535–540
- Cha S, Knopp EA, Johnson G, Wetzel SG, Litt AW, Zagzag D (2002) Intracranial mass lesions: dynamic contrast-enhanced susceptibility-weighted echo-planar perfusion MR imaging. *Radiology* 223(1):11–29
- Kumar VA, Knopp EA, Zagzag D (2010) Magnetic resonance dynamic susceptibility-weighted contrast-enhanced perfusion imaging in the diagnosis of posterior fossa hemangioblastomas and pilocytic astrocytomas: initial results. *J Comput Assist Tomogr* 34(6):825–829. doi:10.1097/RCT.0b013e3181ef77e2
- Cuccurullo L, Prudente ME, Maffia S, Accardo M (2009) An ultrastructural study of the histogenesis of haemangioblastoma. *Pathologica* 101(1):1–5
- Hussein MR (2007) Central nervous system capillary haemangioblastoma: the pathologist's viewpoint. *Int J Exp Pathol* 88(5):311–324. doi:10.1111/j.1365-2613.2007.00535.x
- Uematsu H, Maeda M, Sadato N, Ishimori Y, Matsuda T, Koshimoto Y, Kimura H, Yamada H, Kawamura Y, Takeuchi H, Yonekura Y, Itoh H (2002) Measurement of the vascularity and vascular leakage of gliomas by double-echo dynamic magnetic resonance imaging: a preliminary study. *Investig Radiol* 37(10):571–576. doi:10.1097/01.RL1.0000028483.51109.29
- Paulson ES, Schmainda KM (2008) Comparison of dynamic susceptibility-weighted contrast-enhanced MR methods: recommendations for measuring relative cerebral blood volume in brain tumors. *Radiology* 249(2):601–613. doi:10.1148/radiol.2492071659
- de Fatima Vasco Aragao M, Law M, Batista de Almeida D, Fatterpekar G, Delman B, Bader AS, Pelaez M, Fowkes M, Vieira de Mello R, Moraes Valenca M (2014) Comparison of perfusion, diffusion, and MR spectroscopy between low-grade enhancing pilocytic astrocytomas and high-grade astrocytomas. *AJNR Am J Neuroradiol* 35(8):1495–1502. doi:10.3174/ajnr.A3905
- Law M, Yang S, Babb JS, Knopp EA, Golfinos JG, Zagzag D, Johnson G (2004) Comparison of cerebral blood volume and vascular permeability from dynamic susceptibility contrast-enhanced perfusion MR imaging with glioma grade. *AJNR Am J Neuroradiol* 25(5):746–755
- Kuesel AC, Briere KM, Halliday WC, Sutherland GR, Donnelly SM, Smith IC (1996) Mobile lipid accumulation in necrotic tissue of high grade astrocytomas. *Anticancer Res* 16(3B):1485–1489
- Ishizawa K, Komori T, Hirose T (2005) Stromal cells in hemangioblastoma: neuroectodermal differentiation and morphological similarities to ependymoma. *Pathol Int* 55(7):377–385. doi:10.1111/j.1440-1827.2005.01841.x
- Isobe T, Yamamoto T, Akutsu H, Anno I, Shiigai M, Zaboronok A, Masumoto T, Takano S, Matsumura A (2010) Proton magnetic resonance spectroscopy findings of hemangioblastoma. *Jpn J Radiol* 28(4):318–321. doi:10.1007/s11604-010-0421-5